



CONTROL OF RADIOACTIVE WASTE-GLASS MELTERS: PART 3--GLASS
ELECTRICAL STABILITY*

By

Dennis F. Bickford, R. C. Propst, and M. John Plodinec

E. I. du Pont de Nemours & Co.
Savannah River Laboratory
Aiken, South Carolina 29808

SRL
RECORD COPY

A paper proposed for **publication** and presentation
Advances in Fusion of Glass
American Ceramic Society Annual Meeting
May 1-5, 1988
Cincinnati, OH

*The information contained in this article was developed during the course of work under Contract No. DE-AC09-76SR00001 with the U.S. Department of Energy. By acceptance of this paper, the publisher and/or recipient acknowledges the U.S. Government's right to retain a nonexclusive, royalty-free licence in and to any copyright covering this paper, along with the right to reproduce and to authorize others to reproduce all or part of the copyrighted paper.

CONTROL OF RADIOACTIVE WASTE-GLASS MELTERS:
PART 3 - GLASS ELECTRICAL STABILITY,
D.F. Bickford, R.C. Propst, and M.J. Plodinec,
E.I. du Pont de Nemours & Co.,
Savannah River Laboratory,
Aiken, SC 29808

ABSTRACT

Pilot waste-glass melter operations have indicated a tendency for noble-metal fission-product accumulation on melter floors, which can lead to distortion of electric heating patterns, and decrease melter life. Changes in melter geometry are being considered in Japan, Germany and the United States to permit draining of the noble metals to reduce their effects. Physical modeling of melter electrical patterns, electrode/waste-glass electrochemistry, and non-linear electrical behavior have been evaluated for typical waste-glass. It is concluded that major melter design changes should not be necessary for the U.S. Department of Energy's Defense Waste Processing Facility (DWPF). Top electrodes will not be significantly affected. Minor alterations in melter design, monitoring of electrical characteristics, and adjustment of bottom electrode currents can provide protection from shorting if noble metals accumulate.

INTRODUCTION

Slurry Fed Melters (SFM) are being developed in the United States, Europe and Japan for the conversion of high-level radioactive waste to borosilicate glass for permanent disposal. The high transition metal, noble metal, nitrate, organic, and sulfate contents of these wastes lead to unique melter control requirements. Pilot scale operations have indicated that control of melter physical parameters, as well as glass composition, temperature and redox is necessary for reliable melter operation [1-5].

Waste glasses are semiconductors, and therefore require constant current control, or active control systems to stabilize operating temperature. Any loss of electrical resistance, including the formation of conductive phases, therefore reduces the power available for the melting process.

Waste-Melter Operating Experience with Noble Metals

The Japanese Power and Nuclear Fuel Development Corporation (PNC) produced 3.5 tonnes of simulated waste-glass containing 0.74% RuO_2 , 0.11% Rh, 0.30% Pd, and 0.02% Ag [6]. The waste contained no sulfur. The melter feed was an aqueous slurry of borosilicate glass frit, and formic acid-denitrated waste. At the end of the test, the electrical field in the melter was distorted to the point where glass processing could not continue. The deposits were a mixture of RuO_2 , and alloys of Pd/Te and Ru/Rh. The

concentration ratios of PNC to DWPF feeds are typical of the difference between commercial reprocessing wastes and defense waste (Ru 18:1, Rh 14:1, Pd 1500:1, and Ag 3:1). These results suggest that the DWPF melter could experience significant distortion of power from the bottom electrode pair after about 150 melter throughputs, or about 1.5 year of continuous operation. PNC has conducted melter tests which indicate that the melter floor requires a 45° slope if the deposits are to be collected and tapped off through a bottom drain valve. Alternatively, PNC electrical modeling has indicated that raising the electrodes off of the bottom of the melter by a distance equal to the radius of the melter will assure adequate melter resistance [7].

117 kg of simulated waste glass containing 0.6% noble metals was produced by the United Kingdom Atomic Energy Authority (UKAEA) [8]. During a 3 month melter idling period the effective melter resistance steadily decreased, until further current increases to maintain temperature became impossible. Melter disassembly and examination indicated that the glass adhering to the bottom 4 cm of the electrodes contained about 15.8% Ru. Ru was primarily present as the metal, and associated with tellurium, but some RuO₂ was also detected. Metallographic and mechanical examination of the electrode indicated that this same lower 4 cm region had operated close to the alloy 690 melting point of 1350°C, and small projections at the melter foot had been partially melted, even though the monitored glass temperatures had never exceeded 1150°C. It was concluded that a 4 cm layer of high electrical conductivity glass formed when Ru collected at the melter bottom, and local electrical resistivity dropped as the layer compacted. Low resistance in this area caused power to concentrate at the bottom of the electrodes, resulting in localized overheating, even at low total power.

7.6 tonnes of low enrichment waste concentrate (LEWC) containing 1.5 to 2.2 g/L noble metals were converted into 78 tonnes of waste-glass using a Kernforschungszentrum Karlsruhe (KFK) designed melter in the Deutsche Gesellschaft für Wiederaufarbeitung von Kernbrennstoffen mbH (DKW) PAMELA facility in Belgium [9]. Electrical shorting occurred between bottom electrodes and a bottom drain, causing the drain valve to become inoperable, when the resistance between the bottom electrodes dropped to 10% of its original value. Probing of the glass determined that a 5 cm thick layer at the melter floor was the cause of the shorting. Analysis of samples determined that the bottom glass was 10.4 % RuO₂, 0.05 % PdO, 0.02% Se, 0.02% Te, and 0.25% S. Thus, RuO₂ is believed to be the major cause of the shorting. Sparging of the deposits was partially successful in resuspending and flushing them. Operations are continuing at a reduced production rate, using other electrodes higher in the glass pool.

A series of five melting tests were made at the Battelle Pacific Northwest Laboratory (PNL) with very reducing simulated DWPF melter feeds derived from formate salts [10,3]. Sulfide nodules from the tank floor at the end

of these runs contained 20% of the ruthenium, 25% of the selenium, and 40% of the tellurium fed to the system. The nodule composition was nickel sulfide, Ni_3S_2 , with part of the sulfur replaced by selenium and tellurium. A total of about 45% of the ruthenium fed is believed to have collected at the melter floor, partially as RuO_2 particles. In a similar 30 day long campaign in an engineering scale melter, ruthenium was added as RuO_2 , and feed was prepared with mercury and less reducing agent (formic acid). The resulting glass was not strongly reduced [3], and only small Ru particles 3 to 6 microns in diameter were found on the melter floor. Analysis of the glass concluded that the majority of the ruthenium had remained as finely dispersed RuO_2 , and exited the melter with the glass.

Thus, existing work has established that the presence of noble metals in high level nuclear waste can become a substantial operating problem, which can reduce the production rate and operating life of waste-glass melters. Similar effects can occur from the accumulation of sulfides during operation with reduced waste glass. Melter design features to reduce the problems caused by noble metals in waste glass melters have been reviewed by Chapman et al [11]. The most favored method consists of sloping the melter bottom away from electrodes at steep angles (typically 45° from the horizontal), collecting the unconsolidated and undecontaminated metals in the resulting depression, and either routinely or periodically draining the noble metal rich waste-glass.

The necessity for such approaches to accommodating noble metals is uncertain for the DWPF, since the DWPF wastes are an order of magnitude lower in noble metal content than the commercial reprocessing wastes being studied by most of the mentioned facilities. Such modifications are also very undesirable for the DWPF, since they would require the addition of about one meter to the height of the melter, with corresponding increases in melter mass, and power requirements. The large sump created by a steeply sloped bottom, or a deep well below the bottom electrodes is more difficult to maintain at operating temperatures than flat bottom designs, and could require additional electrodes, and electrical power circuits. Minimum melt rates required by DWPF operating economics have not been demonstrated on this style of melter [1]. Such modifications would also require extensive re-engineering of the coupling devices used for remote maintenance, melter supports, and relocation of auxiliary equipment. Sloping floors also result in undesirable bottom joint geometries, which make refractory construction more difficult and expensive, adversely affect construction times, and could adversely affect refractory life [12].

The mercury and formic acid in simulated DWPF wastes have been found to form amalgams and are therefore expected to affect the agglomeration, settling characteristics, rate of accumulation, and physical properties affecting the electrical conductivity of noble metal deposits [13]. For that reason, extended melter tests of the DWPF melter geometry with noble metal feeds have awaited the construction of the Integrated Demonstration

Melter System (IDMS), which includes equipment for preparing melter feed containing mercury, an offgas system which can control mercury evolution from the melter, and melt cavity and electrode geometry similar to those in the DWPF melter, large enough to give representative results. This report discusses preliminary evaluations, based upon modeling and physical property measurements, to be extended in IDMS operations.

The analyses below are specific to the wastes and melter geometry of the United States Department of Energy's Defense Waste Processing Facility (DWPF), but methods and general conclusions are considered to be applicable to similar wastes and waste-glass melters.

DISCUSSION

WASTE MELTER ELECTRICAL STABILITY CONDITIONS

A joule-heated melter can be thought of as an insulated shell containing one or more pairs of electrodes and molten glass. Molten glass is ionic in character and presents a resistive path to the flow of electric current that produces the heat necessary to evaporate water from slurried melter feed, melt the frit/waste mixture, and maintain the molten glass pool at the operating temperature of 1150°C. Thus, electrical resistivity is a key property in successfully melting waste-glass by the joule effect.

Methods for waste-glass resistivity and thermal diffusivity measurement, and experimental results on simulated waste glass have been discussed earlier [15,16]. Typical values of resistivity are listed in Table I. Waste-glass resistivities vary with composition, are lower than those of commercial glasses, and are typically between 1.8 and 3.6 ohm-cm at 1150°C. Resistivity varies with temperature and composition in a manner similar to viscosity, and can be parameterized by use of the Arrhenius or Fulcher equations.

Analysis of commercial glasses has determined that they are electrically unstable when $1/\rho \, d\rho/dT_a$ is above 0.3 % °C⁻¹, where ρ is the electrical resistivity in ohm-cm, and T_a is the temperature, °K [16]. For waste glass this parameter ranges from 0.26 to 0.65 % °C⁻¹ at 1100 °C, therefore waste glasses are generally expected to require active power control. That is, the waste-glass and melter refractories are semiconductors, which decrease their electrical resistivity as temperature is increased. This results in the effect that perturbations in the electrical current have positive feedback, and can result in unstable conditions. Instabilities of this type are difficult to assess analytically because of the dependency of physical properties on temperature. Finite element analyses based upon typical waste glass properties indicate that the relatively low thermal diffusivity and positive coefficient of electrical conductivity with temperature result in

channeling of the electric current, and localized temperature gradients are typical conditions in waste glass melters [17]. Observation of 25 to 50°C fluctuations in glass temperature readings tends to confirm this. In addition, viewing the top of the melt pool during idling conditions gives a visual indication of local temperature cells about 15 cm diameter, which are clearly visible in the cooler surrounding glass. The waste glasses are more prone to develop local temperature variations than commercial glasses, because their high transition metal content greatly reduces radiative heat transfer in the melt [18], making it more difficult to damp out thermal fluctuations. The effect on melter operating life may also be more severe than in commercial melters because of the small temperature margin for electrode melting [1].

Second Phase Effects on Electrical Resistivity

Three possible sources of second phases in waste glass have been identified which can alter the effective glass electrical resistivity: 1) spinels, 2) noble metals which are present in radioactive waste as fission products, spent catalysts, contaminated equipment, and iodine scrubbers, and 3) precipitates formed by the reduction of sulfates, selenates, or tellurates contained in the wastes.

Spinels Chromia and spinels are a major component of the fuse cast Monofrax K-3 refractory used for glass contact in waste melters. At an operating temperature of 1150°C, the resistivity of Monofrax K-3 is high enough, relative to waste glass, that current flow through the refractory can be ignored. However, at higher operating temperatures conduction through the refractory can become a significant factor. See Table I.

Heavy deposits of spinels were rapidly accumulated in early waste-melter tests (>100 cm / year), with accompanying power losses of 10-20%. Crystalline precipitation is a kinetically limited thermodynamic process, which requires the local glass composition to exceed the solubility, and a nucleating agent or supercooling to proceed. Thus, the precipitation of spinel, phosphates, and similar phases are limited by the waste composition and glass temperature. The similarity in electrical conductivity of spinels and waste-glass minimizes the electrical effect of having a spinel layer on the bottom of an electric melter. Typical waste glasses have higher electrical conductivity than the nickel iron spinel produced when waste glasses are cooled [14,5]. See Table I. Thus, the greatest concern with spinels is that they will cause electrical current flow to shift away from the bottom of the melter, resulting in a cooler bottom, and accelerated spinel accumulation. Spinel does not accumulate in melters with minimum temperatures limits above the liquidus. Accumulation has been controlled to less than 1 cm / year through glass formulation, slurry feeding and maintenance of melt temperatures above the liquidus [19]. Spinel will not be discussed further because they can be controlled,

cause only minor shifts in electrical paths, and can be redissolved in dilute waste glass if necessary.

Noble Metals The noble metals have very limited solubility in molten waste glass. Ruthenium is the major concern because it is the most abundant noble metal fission product. Ruthenium's glass solubility is below the limit of detection (0.001 wt%) and is generally found as RuO_2 [4,5,20]. RuO_2 has been found to have an electrical conductivity of 1.8 to 120×10^{-4} ohm cm at 500°C , with a temperature coefficient of -1.7 to $+0.2 \times 10^{-6}$ ohm cm K^{-1} [21], making it one of the most conductive metal oxides, and giving it negligible resistance when compared to waste glass. Negligible solubilities are expected for palladium and rhodium fission products, because of their chemical similarity to ruthenium. Palladium and rhodium oxides are also less stable at melter operating conditions than those of ruthenium. Thus, the electrical effect of noble metals is considered to be more dependent upon how the noble metals are distributed and agglomerated than on their chemical form.

Silver and Sulfides Silver, silver alloys and sulfides are all similar in that they are molten at nominal melter temperatures, and have negligible electrical resistance when compared to waste glass. Silver has too high an atomic mass to be an abundant fission product, but enters high-level waste as silver catalysts, and iodide scrubbers. Silver will dissolve to a limited extent in waste glass, providing the glass is not very reduced [22]. Thus, silver may be dissolved in waste glass by keeping its concentration low, and the glass relatively oxidized. Similarly, sulfides can be oxidized to sulfates, and dissolved in oxidized waste glass. The oxygen fugacity for sulfide/sulfate transition in waste glass has been reported by Schreiber et al [23]. Glass oxygen fugacity can be measured by determining glass ferrous/ferric ratios [24,25], and comparing the results to published graphs [26-29]. Oxygen fugacity control can then be accomplished by balancing the oxidizing and reducing species [1,3].

LINEAR ELECTRICAL MODELING OF SECOND PHASE ACCUMULATION

Two-dimensional electrical models have been analyzed to determine what design features are necessary to maintain DWPF melter operations with conductive precipitates present on the melter floor. Figure 1 indicates the melter geometry, with two pairs of diagonally opposed electrodes. The models simulated a vertical cross section of the melter using the electrically conductive paper method discussed by Stanek [30]. The method was improved for this study by adding a series of copper strips connected by electrical resistors to simulate different relative conductivities of a high conductivity layer on the melter floor. The top of Figure 2 shows the results of these studies, where a layer of uniform conductivity is assumed at the bottom of the DWPF melter. The layer's electrical properties are indicated by a parameter defined by combining the thickness of the

accumulated layer, and the effect on electrical conductivity: the layer's thickness in centimeters is multiplied by the ratio of the layer's conductivity to the conductivity of the normal glass. The various lines indicate the impedance between electrode pairs. Thus, the line labeled TOP is the impedance between the top electrode pair, DIAGONAL is the impedance between the top electrode on one side and the bottom electrode on the opposite side. VERTICAL is the impedance between electrodes on the same side of the melter, and LINKED is the impedance where electrodes on the same side have been connected together. Impedances shown are the actual ones for the model, and have not been adjusted for the resistivity of glass.

Based upon data shown in the top half of Figure 2, a factor of 10 cm increase in conductivity parameter (i.e. 1 on the \log_{10} scale) of the layer might not be detected since the true RMS electrical meters on the DWPF melter are accurate to 5%. A layer with a conductivity parameter of 100 cm (i.e. 2 on the \log_{10} scale) would be detectable, but could easily be confused for a temperature or glass composition effect, particularly if it developed slowly over a period of time, since the normal range of waste glass resistivity is of the same order of magnitude. A layer with a conductivity parameter of 1000 cm (i.e. 3 on the \log_{10} scale) corresponds approximately to that which resulted in electrode loss in the PAMELA facility. By the time a layer with a conductivity parameter of 10 000 cm has accumulated, the bottom electrodes are virtually shorted, and negligible power can be generated by passing current between the bottom electrodes.

As the line labeled DIAGONAL indicates, in the event of large amounts of noble metal accumulation, there are significant advantages to the alternative, diagonal arrangement for electrode connection. First, this arrangement would maintain the ability of both power supplies to input power into the melt, maintaining redundancy. Second, it would generate the power relatively low in the melt, helping to sustain the convection necessary for rapid melting, and maintenance of temperature near the floor of the melter. Third, this arrangement might prevent electrode loss by assuring that impedance does not fall below that of the path between top and bottom electrodes, labeled VERTICAL in Figure 2.

In the bottom half of Figure 2, the various electrode pair resistances are plotted relative to the bottom pair resistance, to decrease the sensitivity of this detection method to bulk resistivity shifts. By this method it should be possible to clearly distinguish between power losses resulting from a conductive layer, and those resulting from glass temperature and composition changes. It is therefore proposed that similar measurements be made at regular intervals whenever noble metals are being processed in waste-glass melters. This should probably be done under relatively uniform conditions, such as during melter idling periods, at one established

temperature. It may also be possible to improve the sensitivity of this method by compensating for any known shifts in the bulk conductivity.

Silver, Silver/Noble Metal Alloys and Sulfides Silver, silver/ noble metal alloys and sulfides are similar to noble metals in their effects, since they are dense and electrically highly conductive. They are different in that their melting points are below the nominal glass operating temperature, and can therefore form molten nodules or puddles at low points in melters. These, and the related selenide and telluride compounds will be referred to as sulfides in the following discussions. Whereas noble metal effects are limited by the amount of contact between particles, it is most probable that the direct effects of sulfides are limited only by the melter geometry, and the amount of material precipitated. Indirect effects could include accelerated electrode and drain valve corrosion, which will not be discussed here. Thus, a different set of models was required to investigate the possible effects of sulfide accumulation on melter electrical behavior. Figure 3 shows the results of the modeling. Electrode pairs are identified the same as with the previously described models, except that horizontal (plan view) models have been added, labeled PLAN. By following the electrical response of a single electrode pair, it is not likely that the sulfide accumulation would be detected from the voltage and current levels until 30 to 50% of the gap between the bottom electrodes is bridged by the sulfide. Thus it is possible to deliberately operate the DWPF melter with a sulfide or molten metal layer while allowing some power to the bottom electrodes, but control of the size of the puddle is critical for the existing DWPF melter design. Top electrode currents are relatively unaffected by sulfides, and would remain available for final draining, or operation at reduced production rate.

An increase in the elevation of the bottom surface of the bottom electrode is desirable to increase the size of the molten pool, or the extent of high electrical conductivity noble metal precipitation which can be accommodated without bottom electrode shorting. Figure 3 presents the data from a series of models used to investigate the sensitivity of bottom electrode resistance to bottom electrode elevation. The data indicates that lowering the melter bottom by 10 to 25% of the electrode gap (about 10% of melter diameter) is the practical range to prevent excessive shorting. The optimum height is about 20% of the gap between bottom electrodes, with adequate additional height to account for the depth of noble metal or sulfide accumulation. That is, it is not necessary to lower the melter floor by the melter radius to achieve most of the benefits of raised electrodes. The sensitivity of the ratioed resistances shown in the bottom of Figure 4 is not significantly different from the corresponding shifts in the electrode impedances, but again, the use of ratios to compensate for temperature and bulk conductivity effects should make the use of ratios a more reliable means of determining the actual height of the bottom electrode above the conductive layer.

NONLINEAR ELECTRICAL BEHAVIOR OF SIMULATED WASTE GLASS

Electrical resistivity and electrochemical measurements were conducted on simulated waste-glass to determine the limitations caused by the assumption of electrical linearity in the 2 dimensional electrical modeling discussed above. Tests consisted of determination of the errors caused by non-ideal glass/electrode contact resistance, breakdown of ionic conduction at high current densities, and estimation of the tendency for waste glass to form high temperature channels, which could lead to excessive local temperatures.

Electrode to glass contact resistivity results are shown in Table IV. Resistivity test equipment and methods have been described earlier [15]. The observed behavior of the resistive and capacitive terms are in general agreement with those predicted by electrochemical theory, which predicts that the resistive term should decrease and the capacitive term should increase as the current density is increased. Except for the the lowest current values, this is the general behavior observed in Table II. Based on these measurements, the electrode to glass contact resistance for a full scale melter is negligible, and contact capacitance is extremely large. Both results are highly desirable from the stand point of melter design, indicating that transfer of current from electrode to glass is a negligible source of error in the models.

Details of the electrochemistry of electrode attack were examined by adding a Pt reference electrode, a waveform generator, potentiostat, and oscilloscope to the resistance measurement apparatus. Cyclic voltammetry was conducted with sodium silicate, lithium silicate and lithium metaborate standards, as well as simulated waste glass at 0.05 to 60 Hz. It was concluded that cathodic charge transfer at the electrodes is associated with the reduction of alkali oxides. When the AC cycle reverses, the alkali is reoxidized to transfer the anodic current. However, when DC biases, or low frequency alternating currents are applied, alkalis are reduced at the cathode, and boil off. Under these low frequency conditions, at low boundary layer voltages, the only corresponding anodic reaction is electrode oxidation, e.g. Cr^0 to Cr^{+3} . When extraordinarily high DC biases of 8.2 to 9.2 volts are applied, the oxidation proceeds to Cr^{+6} , which volatilizes, and visible electrical discharge occurs. There is no plausible source of such high biases in waste melters, which typically have 60 Hz total voltage drop 50 V. In the DWPF, DC current sensing, alarms and interlocks give assurance that neither anodic dissolution of electrodes, nor arcing will occur.

Laboratory melter tests were conducted, and previous tests reviewed for comparison to the electrochemical tests, to determine practical limitations on waste melter current density. Minimum test time was one month. The waste

glass consisted of 42.0% SiO₂, 8.0% B₂O₃, 3.2% Li₂O, 15.2% Na₂O, 5.1% CaO, 14.5% Fe₂O₃, 3.8% MnO₂, 3.2% Al₂O₃, 2.8% zeolite, 1.7% NiO, and 0.4% Na₂SO₄. Results are shown in Table III. It was concluded that alloy 690 electrode corrosion rate has little dependence upon either temperature or AC current density. Alternating current densities as high as 25 amperes cm⁻² in these small melters did not show any major effect, indicating that the 0.5 ampere cm⁻² design criteria used for the DWPF melter is very conservative. In the same tests, however, it was determined that DC voltage differences as low as 0.12 to 0.22 V between electrodes result in electrolysis, anodic electrode attack, and O₂ evolution, all of which are in excellent agreement with laboratory electrochemical tests.

Given the tendency for current to channel through waste glass, it is necessary to perform bounding calculations on localized current density to quantify when localized over heating can occur while average currents are kept low. A conservative bounding calculation can be performed for normal current flow between electrodes, by estimating the current carried by the channel, and assuming that electrodes can experience damage when the glass temperature adjacent to any point on the electrode exceeds the alloy 690 melting point of 1350°C. Steady state heat transfer can then be modeled as a conducting cylinder inside of a uniform temperature glass pool. For this geometry, integration of the energy flux equation, and substitution of Fourier's law over a limited temperature range yields the solution:

$$T_{\max} - T_o = I_{cd}^2 R^2 \rho (4k)^{-1} \quad (1)$$

Where $T_{\max} = 1350^\circ\text{C}$, T_o is the glass pool temperature, I_{cd} is the current density (amps cm⁻²), R is the radius of the cylindrical channel, ρ is resistivity (ohm-cm), and k is the thermal conductivity [31]. By definition:

$$I_{cd}^2 = (I_c (\pi R^2)^{-1})^2 = I_c^2 \pi^{-2} R^{-4} \quad (2)$$

where I_c is the total channel current (amps). Substitution of (2) into (1), and solution for I_c yields:

$$I_c = 2\pi R ((T_{\max} - T_o) k / \rho)^{0.5} \quad (3)$$

Alternatively, rearrangement and solution of (1) for the critical current density (I_{ccd}) yields:

$$I_{ccd} = I_c / \text{Area} = 2R^{-1} ((T_{\max} - T_o) k / \rho)^{0.5} \quad (4)$$

To the first order the error introduced (by assuming that the electrical and thermal diffusivities are constant) can be recovered by substituting the values for k and ρ at the average temperature into these equations. For this geometry the cross-sectional-area-averaged temperature for the channel is the arithmetic mean of T_{\max} and T_0 [31].

Table IV includes the calculated total channel current as a function of nominal glass temperature, and radius of the channel, together with the corresponding average current density in the channel.

The channel current will remain stable if the current through the bulk of the glass establishes the voltage drop necessary to sustain the channel current, since the melter systems are operated at constant current. If the channel current path length is the same as the electrode gap distance, then the current through the bulk glass (I_{bulk}) necessary to sustain the critical channel current can be determined by equating their voltage gradients:

$$dV/dx = \rho_{\text{bulk}} I_{\text{bulk}} (\text{Area}_{\text{electrode}})^{-1} = \rho_{\text{channel}} I_c (\pi R^2)^{-1} \quad (5)$$

which can be solved for I_{bulk} . Table X includes the calculated bulk current to sustain the critical channel current. If the actual electrode current is less than the sum of I_{bulk} and I_c , then the channel will partially collapse, and the critical temperature of 1350°C will not be exceeded locally in the glass. If the actual current is higher, then the channel will grow, and the critical temperature will be exceeded only as a limited core through the center of the channel. It is important to remember that this analysis is also conservative because it does not take any credit for the ability of the electrode to cool the glass adjacent to it, for the high thermal conductivity electrode to dissipate local temperature gradients, or for the ability of the electrodes' top and bottom surfaces to conduct to the glass.

The critical current density in the channel, I_{ccd} , is well below the current densities which have been demonstrated experimentally in Table II and III, giving confidence that no unexpected electrode deterioration will occur. Similarly, the total electrode current, the sum of I_c and I_{bulk} , is compatible with the 0.5 amp cm⁻² design rating for the 2800 cm² surface area of the bottom electrodes, i.e. 1400 amperes.

The calculated electrode current can be applied to the condition where conductive sulfide deposits have accumulated on the melter bottom, or the melter floor has been lowered, and conductive layers have accumulated. In this case the assumption that the channel currents' path is the same as the electrode gap is no longer valid, and the I_{bulk} must be derated by the ratio of the electrode gap to the shortest possible channel current path. For instabilities adjacent to a refractory wall or floor, the refractory

can be considered to be a perfect insulator, and by symmetry the critical channel current will be one half the value of Table IV, but I_{bulk} is unaffected.

For the accumulation of loosely agglomerated noble metals, it is reasonable to assume that the presence of the noble metals has proportional effect on both the electrical and the thermal conductivity. Thus, since electrical conductivity is the inverse of electrical resistivity, the critical total current described by equation 3 is expected to increase proportional to the relative increase of electrical conductivity caused by noble metal, with no effect on I_{bulk} , except those described by the 2 dimensional models.

SUMMARY AND CONCLUSIONS

Electrochemical studies of electrode to glass contact and operations with small melters indicate that electrode current densities can be at least an order of magnitude higher than DWPF design criteria, but relatively small DC currents can lead to accelerated electrode wear. For very large melters the total current between electrodes is limited by the tendency of waste glass to form high temperature channels, rather than the average current density. Conservative methods of estimating this effect are presented.

The DWPF melter is susceptible to derating of the bottom electrodes if noble metal fission products accumulate on the melter bottom. Modeling and experience confirm that the effect will be detectable and quantifiable before damage to the bottom electrodes occurs. A means of derating the bottom electrode current carrying capacity has been presented, to avoid localized overheating of the electrodes. In the event of significant derating of the bottom electrodes, modeling indicates that top electrodes would not experience significant loss of power, and would remain available for further processing at slower production rates, and for final draining.

The ratioing of the apparent resistance of electrode pairs permits the compensation for average temperature and glass composition effects on glass resistivity, increasing the sensitivity of monitoring for and quantifying noble metal accumulation.

Modeling further indicates that for waste melters the optimum distance from the bottom surface of bottom electrodes, to the top surface of deposited noble metals, silver alloys or sulfides is about 20% of the gap between bottom electrodes. The practical limits are about 10 to 25% of the gap. In the presence of noble metal or sulfide accumulation, raised bottom electrodes can continue to be operated, but must be derated to account for the short path that channel currents can follow between the deposits and the electrodes.

In the event of significant noble metal accumulation in melters with electrodes on the melter floor, diagonal firing from the top electrodes to the opposite bottom electrodes can permit the retention of redundant circuits, and will partially restore melter production capacity.

Duplication of this modeling, using 3-D finite element analysis can be expected to improve both the reliability and accuracy of the analysis, since it would permit more detailed simulation of melter geometry, glass convection effects, and electrode temperature gradients.

ACKNOWLEDGEMENTS

This paper was prepared in connection with work done under contract No. DE-AC09-76SR00001 with the US Department of Energy. Monofrax K-3 is a trademark of SOHIO Engineered Materials Company.

REFERENCES

- [1] D.F. Bickford, P. Hrma, B.W. Bowen, and P.K. Smith, "Control Requirements for Radioactive Waste Glass Melters-Parts 1 & 2", submitted Am. Cer. Soc. 1987.
- [2] D.S. Goldman, "Melt Foaming, Foam Stability and Redox in Nuclear Waste Vitrification", J. Non-Cryst. Solids 84 (1986) 292-298.
- [3] D.F. Bickford, R.B. Diemer, and D.C. Iverson, "Redox Control of Electric Melters with Complex Feed Compositions, Parts I & II", J. Non-Crystalline Solids, 84(1986) 276-291.
- [4] D.F. Bickford and C.M. Jantzen, "Devitrification of Defense Nuclear Waste Glasses: Role of Melt Insolubles", J. Non-Crystalline Solids 84 (1986) 299-307.
- [5] C.M. Jantzen, D.F. Bickford and D. G. Karraker, "Time-Temperature-Transformation Kinetics in SRL Waste Glass", Advances in Ceramics, Vol 8 (1984).
- [6] N. Sasaki, et al, "Solidification of the High-Level Liquid Waste from the Tokai Reprocessing Plant", ANS Inter. Meeting Fuel Reprocessing & Waste Man., Jackson WY, August, 1984.
- [7] M. Yoshioka, Japanese Power and Nuclear Fuel Development Corp., private communication, 1987.
- [8] J.B. Morris, et al, "Electrode Corrosion and Ruthenium Behavior in a Small Joule Ceramic Melter", AERE R 12349, October 1986.
- [9] M. Stehle, Deutsche Gesellschaft fur Wiederaufarbeitung von Kernbrennstoffen mbH (DKW), Presentation at PNL, April, 1987.
- [10] R.W. Goles and G.J. Sevigny, "Off Gas Characteristics of Defense Waste Vitrification,...", PNL-4819, September 1983.
- [11] C.C. Chapman, J.M. Pope and S. M. Barnes, "Electric Melting of Nuclear Waste Glasses: State of the Art", J. Non-Cryst. Solids 84 (1986) 226-240.
- [12] J.M. Ferketic, SOHIO Engineered Materials Co., private communication, 1987.
- [13] D.F. Bickford, H.L. Hull, and R.E. Eibling, "Control of Radioactive Waste-Glass Melters: Part 4 - Physical Chemistry of Noble Metal Deposits", to be issued.
- [14] M.J. Plodinec and J.R. Wiley, "Viscosity and Electrical Conductivity of Glass Melters as a Function of Waste Composition", Ceramics in Nuclear Waste Management, 1979, 210-212.
- [15] R. C. Propst, et al, "Electrochemical Studies of Molten Glass Specific Resistivity Measurements, DP-1677, December 1983.
- [16] A. Andrusieczko, Szklo i ceramika XVI (1965) 209.

- [17] D.W. Pepper, "Recirculation Within a Glass Mixture Subjected to External and Resistive Heating", Fourth Intenat. Conf. Num. Meth. in Laminar and Turb. Flow, Swansea UK, July, 1985.
- [18] D.F. Bickford, L.D. Pye, et al, "Measured Physical properties of Waste Glass", Doe Report OSTI/DPST-85-397, March 1985.
- [19] D.C. Iverson and D.F. Bickford, "Evaluation of Materials Performance in a Large Scale Glass Melter After Two Years of Vitrifying Simulated SRP Defense Waste", Mat. Res. Soc. Symp. Proc. Vol 44 (1985).
- [20] H.D. Schreiber, et al, "Ruthenium in Glass-Forming Borosilicate Melts", J. Less-Common Metals, 115 (1986) 145-154.
- [21] S. Trasatti and G. Lodi, "Properties of Conductive Transition Metal Oxides with Rutile-Type Structure", S. Trasatti, ed., Electrodes of Conductive Metallic Oxides, Elsevier (1980) 301-359.
- [22] H.D. Schreiber, et al, "An Electromotive Force Series in a Borosilicate Glass-Forming Melt", J. Am. Cer. Soc., Vol 67, June 1984, C106-C108.
- [23] H.D. Schreiber, "Sulfur Chemistry in a Borosilicate Melt, Part I: Redox Equilibria and Solubility", Virginia Military Institute Report, January 1987.
- [24] D.S. Goldman, "Investigation of Potential Analytical Methods for Redox Control of the Vitrification Process" PNL -5581/UC-70, November 1985.
- [25] E.W. Baumann, et al, "Colorimetric Determination of Fe(II)/Fe(III) Ratio in Glass", SRL Report DP-MS-87-18, August 1987.
- [26] H.D. Schreiber, et al, "Precipitation of Iron, Cobalt and Nickel Metal from a Borosilicate Glass Melt", XIII Int Cong. Glass, July 1983, Hamburg FRG.
- [27] H.D. Schreiber and G. B. Balazs, "An Electromotive Force Series for Redox Couples in a Borosilicate Melt: The Basis for Electron Exchange Interactions of the Redox Couples", J. Non-Crystalline Solids 71 (1985) 59-67.
- [28] H.D. Schreiber, and A. L. Hockman, "Redox Chemistry in Candidate Glasses for Nuclear Waste Immobilization" submitted to J. Am. Cer. Soc., 1986.
- [29] H.D. Schreiber, et al, "Redox Equilibria and Kinetics of Iron in a Borosilicate Glass-Forming Melt", J. Non-Crystalline Solids 84 (1986) 186-195.
- [30] J. Stanek, "Theoretical and Practical Achievements in the Electric Melting of Glass", J. Non-Crystalline Solids 84 (1986) 353-362.
- [31] R.B. Bird, W.E. Stuart, and E.N. Lightfoot, Transport Phenomena, J. Wiley & Sons, 1960, 271.

TABLE I
TYPICAL WASTE MELTER ELECTRICAL RESISTIVITY RELATIONSHIPS

ELECTRICAL RESISTIVITY, ρ OHM-CM [15]

TEMP, °C	<u>SRL165</u>	<u>SRL165HiFe</u>	<u>W.GLASS</u>	<u>SPINEL</u>	<u>MONOFRAX K3</u>
800	27	19	18.3	43.4	2680
900	13	9.3	9.7	20.1	859
1000	7.1	5.4	5.6	10.5	329
1100	4.4	3.5	3.6	6.0	145
1150	3.6	2.9	2.9	4.7	100
1200	3.0	2.5	2.4	3.7	71
1300*			1.7	2.4	38
1400*			1.2	1.7	22

See Reference 15 for glass compositions.

* data extrapolated using Fulcher Equation

TABLE II
ELECTRODE/WASTE-GLASS CONTACT IMPEDENCE MEASUREMENTS
SERIES RESISTOR AND CAPACITOR IMPEDENCE MODEL AT 1000°C AND 60 Hz.

<u>Electrode</u>	<u>Waste-Glass</u>	<u>Current</u> Amp cm ⁻²	<u>Resistive</u> Ohm cm ⁻²	<u>Capacitive</u> Farad-radian cm ⁻²
Alloy 671	Frit131	1.50	0.46	6.5
Alloy 671	Frit165	1.77	1.02	2.94
Alloy 690	Frit131	0.1	1.71	0.63
Alloy 690	Frit165	0.87	2.30	1.10
Alloy 690	SRL165*	1.92	0.56	4.42
Alloy 690	SRL165*	0.50	0.72	2.50
Alloy 690	SRL165*	1.44	0.67	2.70
Alloy 690	SRL165*	2.21	0.67	2.92
Alloy 690	SRL165*	11.60	0.21	9.58
Alloy 690	SRL165*	20.79	0.19	11.7
Alloy 690	SRL165	0.34	0.14	8.75
Alloy 690	SRL165	0.83	1.30	1.17
Alloy 690	SRL165	2.71	1.06	1.92
Alloy 690	SRL165	5.10	0.72	3.13
Platinum	SRL165	0.23	0.17	2.5
Platinum	SRL165	0.59	0.16	2.5
Platinum	SRL165	6.15	0.09	3.4
Platinum	SRL165	8.95	0.13	3.5

* Simulated average waste glass with formic acid reducing agent and nitrogen cover gas.

TABLE III
CORROSION RATE OF ALLOY 690 BY SIMULATED WASTE GLASS

<u>Metal Temp.</u> °C	<u>Maximum Penetration Rate</u> cm y ⁻¹	<u>Current Density</u> Ampere cm ⁻²
1130-1170	1.26	2.0
1130-1170	1.59	2.0
950-1050	1.47	3.4
1000-1050	1.20	4.5
950-1050	0.74	5.0
1000-1050	1.21	25.0

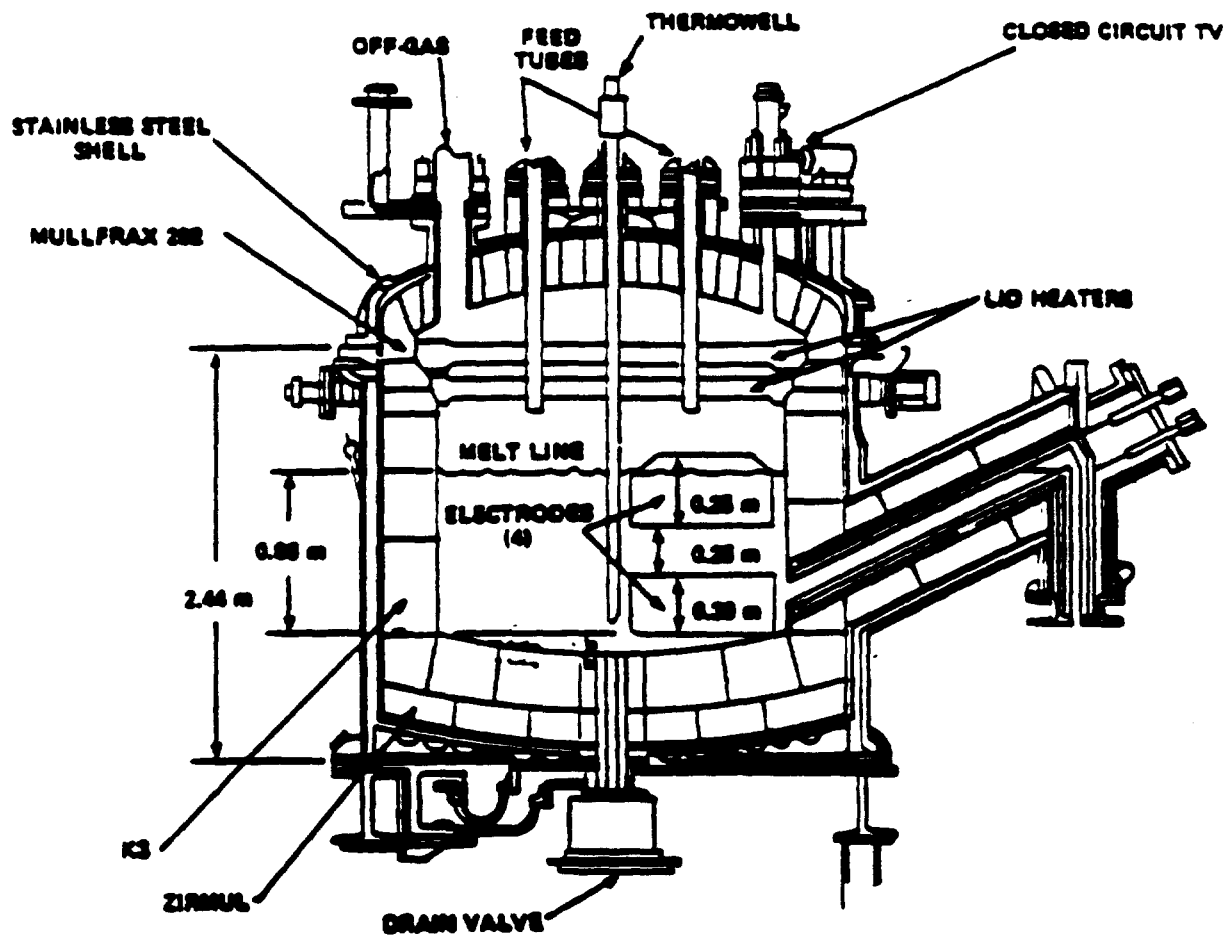
TABLE IV

TYPICAL THERMOPHYSICAL PROPERTIES AND CALCULATED CRITICAL CURRENTS IN WASTE-GLASS

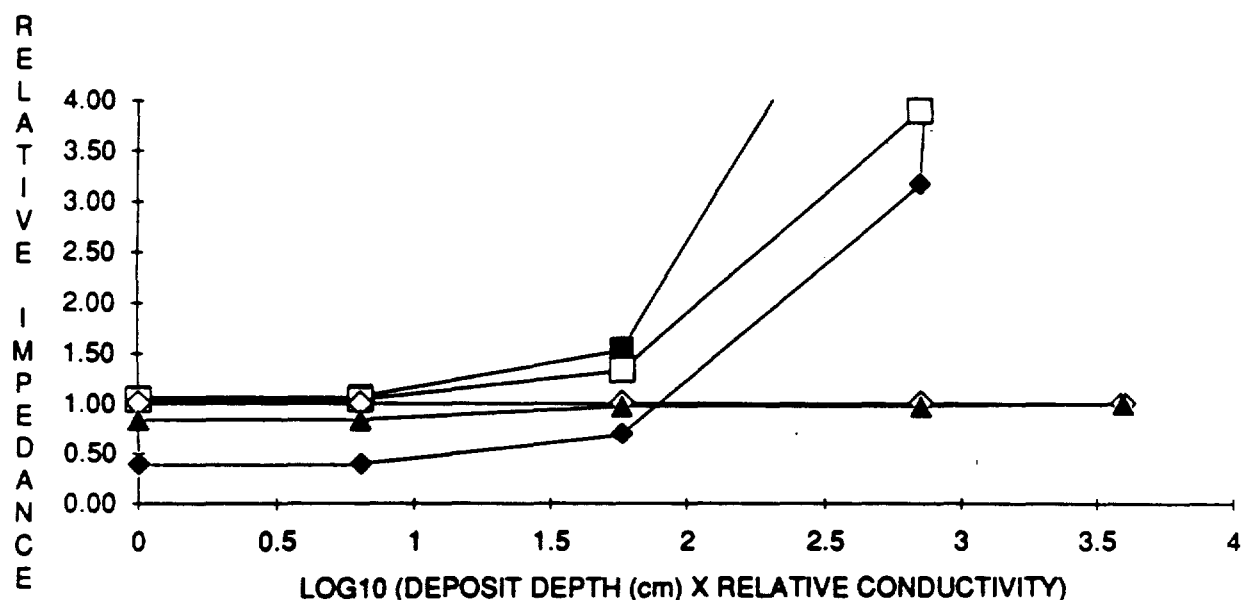
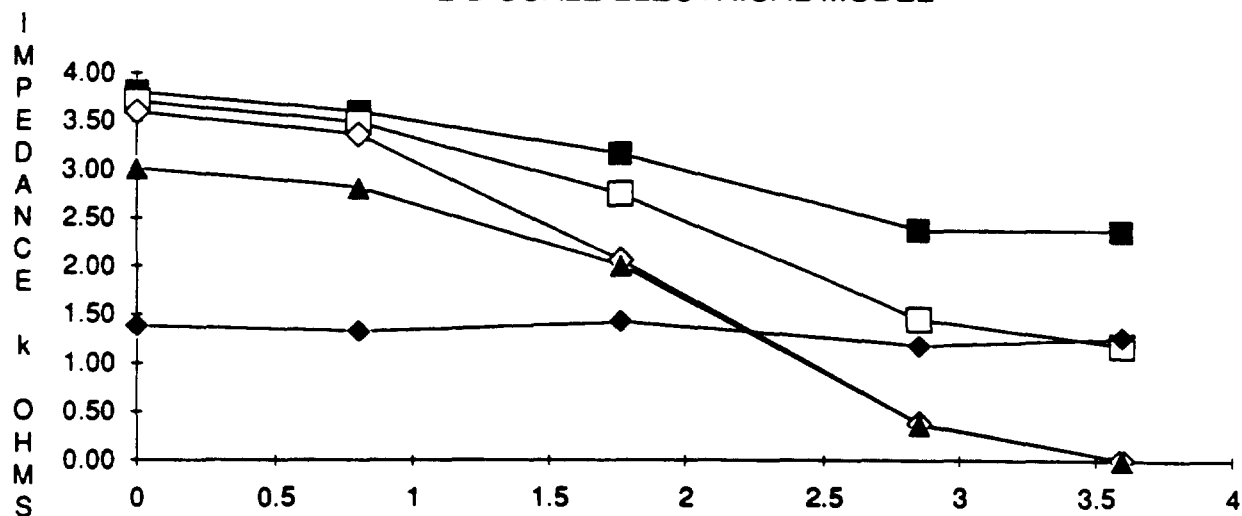
T_o °C	ρ ohm-cm	α cm ² /s	density g/cc	k w/cm°C
800	18.75	0.05	2.65	0.13
850	12.92	0.05	2.63	0.14
900	9.32	0.06	2.61	0.16
950	6.99	0.06	2.59	0.17
1000	5.42	0.07	2.58	0.19
1050	4.31	0.08	2.56	0.21
1100	3.51	0.08	2.54	0.22
1150	2.92	0.09	2.52	0.24
1200	2.46	0.10	2.51	0.26
1250*	2.11	0.11	2.49	0.28
1300*	1.83	0.12	2.47	0.30
1350*	1.61	0.13	2.45	0.32

T_o °C	<u>Channel Radius = 10 cm</u>			<u>Channel Radius = 7.5 cm</u>			<u>Channel Radius = 5 cm</u>		
	I_{ccd} amp/cm ²	I_c amp	I_{bulk} amp	I_{ccd} amp/cm ²	I_c amp	I_{bulk} amp	I_{ccd} amp/cm ²	I_c amp	I_{bulk} amp
800	1.12	351	653	1.49	263	871	2.23	175	1306
850	1.14	359	878	1.52	269	1170	2.28	179	1755
900	1.15	364	1121	1.54	273	1495	2.32	182	2243
950	1.16	366	1373	1.55	274	1830	2.33	183	2745
1000	1.16	364	1616	1.54	273	2155	2.32	182	3233
1050	1.14	357	1836	1.52	268	2448	2.27	179	3672
1100	1.10	345	2013	1.46	259	2684	2.20	172	4025
1150	1.04	326	2122	1.38	244	2829	2.07	163	4244
1200	0.95	297	2132	1.26	223	2843	1.89	149	4264
1250*	0.81	255	1992	1.08	191	2656	1.62	127	3985
1300*	0.60	189	1593	0.80	142	2124	1.20	95	3186

* extrapolated



EFFECT OF CONDUCTIVE LAYER ON IMPEDANCE OF DWPF 2-D SCALE ELECTRICAL MODEL



EFFECT OF SULFIDE ON ELECTRODE IMPEDANCE
DWPF 2-D SCALE ELECTRICAL MODEL

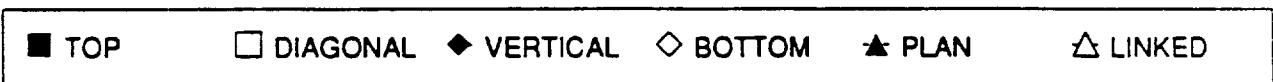
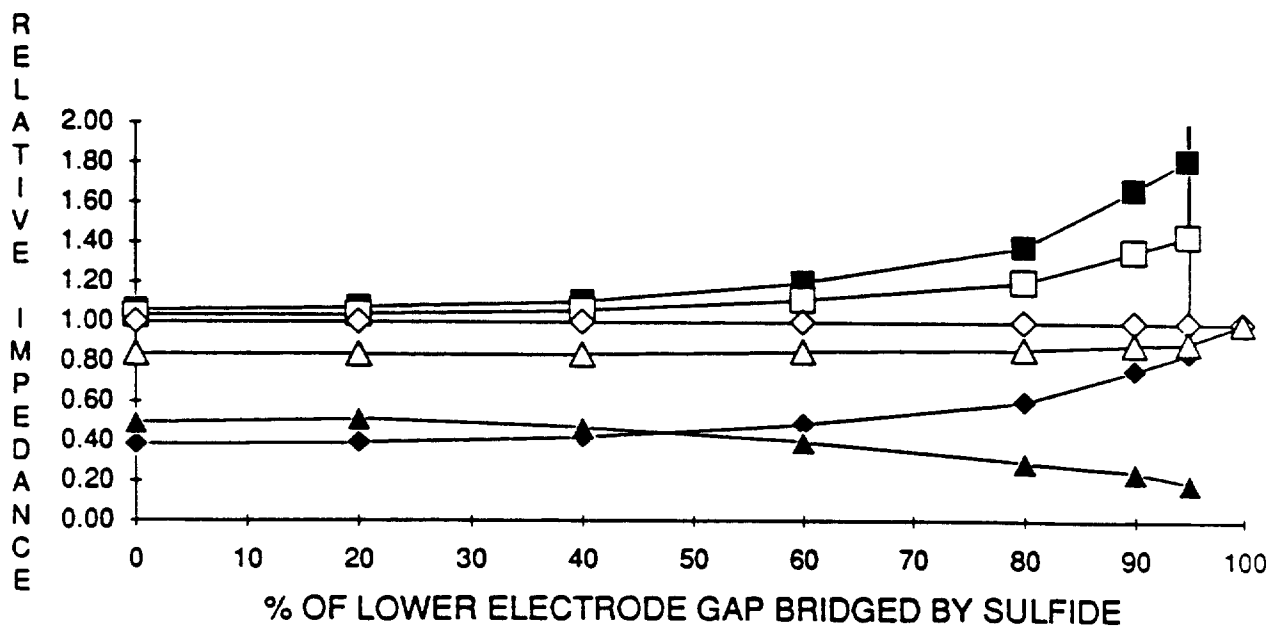
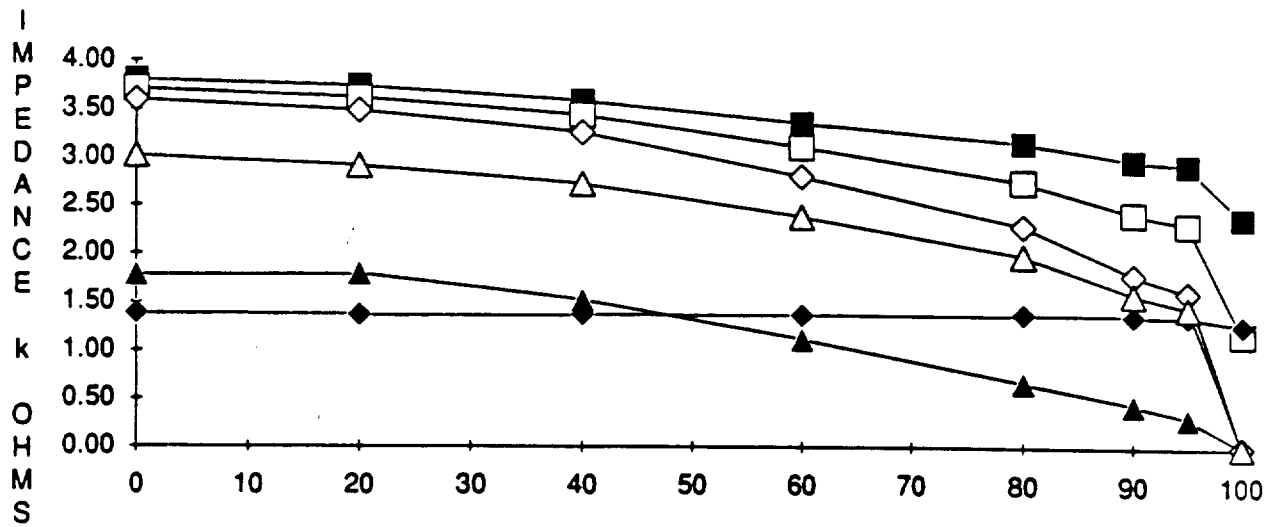


Figure 3

EFFECT OF ALTERING BOTTOM ELECTRODE ELEVATION IN THE PRESENCE OF NOBLE METAL OR SULFIDE

